Identification of a Control-oriented Energy Model for a System of Fan Coil Units

Anita Martinčević[a*], Mario Vašak[b] and Vinko Lešić[c]
[abc] University of Zagreb, Faculty of Electrical Engineering and Computing
Laboratory for Renewable Energy Systems (url: www.lares.fer.hr)
Unska 3, HR-10000 Zagreb, Croatia
[a]anita.martincevic@fer.hr, [b]mario.vasak@fer.hr, [c]vinko.lesic@fer.hr

***Abstract*—In recent years, application of advanced control, fault detection and diagnosis algorithms for building heating and cooling systems has been intensively investigated with the aim to improve their energy efficiency and bring the buildings sector into the smart city arena. Hindering the trend, hysteresis and proportional-integral-derivative controllers are still a common practice for temperature control in buildings with Fan Coil Units (FCUs). Introduction of more sophisticated controllers for additional savings requires a cost-effective approach for identification of an energy model which accurately resembles thermal and hydraulic performance of a system of FCUs. In the present work, the control-oriented energy model of a system of FCUs is developed and accompanied with replicable, robust and simple methodologies for its identification derived by consolidating the advantages of physical modelling, identification methods and manufacturer's catalogue data. The validity of the developed approach is tested on the 248-office living-lab. The introduced simple and accurate dynamic characterization of energy transmitted from a FCU to zone air fills the gap between thermal and energy management for buildings. This enables implementation of predictive building controls and unleashes significant energy and cost-saving potentials of a smart building in a smart city.**

***Index Terms*—control-oriented fan coil unit model; hydraulic model; electric-hydraulic analogy; thermodynamic fan coil unit model; heat capacity estimation**

I. Introduction

Increasing global energy demand and noticeable effects of irrational energy consumption highlighted the improvement of buildings sector energy efficiency as one of the priorities for ensuring long-term energy security due to its significant share in total annual energy consumption [1], [2]. The systems with the largest potential for improvement of buildings sector energy efficiency, with estimated nearly 60% of overall energy consumption in buildings, are Heating, Ventilation, and Air Conditioning (HVAC) systems [2]. The inherent complexity of HVAC systems with uncertain and time-varying dynamics, as well as the presence of unmeasurable disturbances, present serious challenges for the development of corresponding efficient control, fault detection and diagnosis algorithms. Model Predictive Control (MPC) applied in building management systems has been recognized as one of the most promising solutions to achieve considerable energy savings in buildings with estimated theoretical energy saving potential up to 70% in particular comprehensive applications [3]–[5]. Only recently, MPC has found its place in practice, with experimentally-validated building energy efficiency increase by 15-53% [6]–[10]. The reasons are primarily the difficulties in obtaining a suitable mathematical model of a building and its subsystems. Acquiring of accurate thermal energy data from the controllable thermal sources in building zones is the main prerequisite for identification of accurate building thermal models that transform zone energy input into a temperature output. Some authors coped with the problem by using electric heating [11], [12] to excite the building temperature. However, this is often impractical since most of the commercial and residential buildings have water-based (hydronic) or air-based heating and/or cooling [2].

Fan Coil Units (FCUs) are one of the most common heating/cooling elements found in office buildings today. A FCU consists of a fan and one or more air-water heat exchangers. Multiple FCUs connected in parallel to a common supply line form a system of FCUs. Overall performance of a FCU as a part of the system is described with a hydraulic model characterizing the distribution of the heating/cooling medium through the system and a thermodynamic model for assessment of thermal energy generated by the FCU. In general, thermodynamic heat exchanger models in literature are divided into three groups: *i*) physical models based on a number of transfer units or the logarithmic mean temperature difference relations [13]–[17] or relied on fundamental physical laws, *ii*) non-physical models completely relied on the experimental data and *iii*) semi-physical models as a compromise between the first two groups. Physical models require detailed physical properties of a FCU, such as fin thickness or tube dimensions, which are often omitted from manufacturer's catalogue and are hardly measurable on the final on-site product [18]–[22]. Non-physical models, usually put in a form of simple linear approximations around an operating point [6] or neural networks [23]–[26], decrease in accuracy when operating outside the training range. Semi-physical models exploit physical knowledge or some other a-priori information to specify the model structure while the unknown parameters are identified based on the experimental [27]–[29] or manufacturer's catalogue data [27]. Whilst the experimental analysis of heat exchangers in general is widely elaborated, experimental analysis of a FCU is scarcely considered in only few papers that concern with mainly a single

* Corresponding author
email: anita.martincevic@fer.hr, *phone*: +38516129893

NOMENCLATURE

Symbols

α	exponent of pressure drop charachteristics
β	exponent of U_o function
Δh	change in pipe elevation [m]
Δp	pressure drop [Pa]
η	flow share through an individual FCU [%]
μ	dynamic viscosity [Pa·s]
ϕ	heat transfer coefficient [K^{-1}]
$\boldsymbol{\varepsilon}$	set of coefficients of U_o function
ρ	density [$\mathrm{kg{\cdot}m}^{-3}$]
τ	Transport delay [s]
$\mathbf{a}$	set of coefficients of U_o function
$\mathbf{b}$	set of coefficients of U_o function
c	specific heat capacity [$\mathrm{J{\cdot}(kg{\cdot}K)}^{-1}$]
d	diameter [m]
f_D	friction coefficient
g	acceleration of gravity [$9.81\ \mathrm{m \cdot s}^{-2}$]
i	FCU index $i = 1, \ldots, n$
l	length [m]
m	mass [kg]
N	number of zones supplied through the considered duct
n	number of FCUs connected to the same duct
P	power [W]
q	mass flow [$\mathrm{kg{\cdot}s}^{-1}$]
R	hydraulic resistance
Re	Reynolds number
T	temperature [^{o}C]
U_o	overall heat transfer coefficient [$\mathrm{W{\cdot}K}^{-1}$]
x	fan speed $x \in \{\mathrm{off}, \mathrm{L}, \mathrm{M}, \mathrm{H}\}$
H	high fan speed
L	low fan speed
M	medium fan speed
off	fan switched off

Superscripts

a	a-priori
c	calibrated measurement
cd	manufacturer's catalogue data
in	input
m	measured value
out	output
raw	raw measurement
s	supply
x	associated with a certain fan speed x

Subscripts

a	air
cal	calorimeter
fc	fan coil unit
p	pipe
w	water

FCU [6], [30]. The thermodynamic performance of a FCU depends on thermal properties of the heating/cooling medium used within the system of FCUs. Most hydronic systems in buildings use softened tap water or water-glycol mixtures as a working fluid with rarely known accurate thermal properties. To the best of the authors' knowledge, this issue is not covered when discussing modelling of heat exchangers.

While thermodynamic model of a single FCU can be easily assessed if measurements of the medium flow through the unit as well as measurements of supply and return medium and air temperatures are available, such information is often unavailable for a system of FCUs. To be able to determine unknown flow through a certain FCU, based on one central measurement of the flow through the system, a hydraulic model of the system is required. Use of the hydraulic model for the system design and subsequently its management significantly reduces operating costs [31], [32]. Inclusion of both, hydraulic and thermodynamic model into the building management system offers further savings by enabling dynamic flow control with respect to the thermal demands per zones [33]. A hydraulic performance of a FCU and sensors-free solution for determining the medium flow through the unit is rarely discussed. Authors of [34] suggest using pressure drop sensors to determine the flow through the heat exchanger. However, this tends to be cost-intensive when applied to individual FCUs due to a large number of expensive sensors required and corresponding installation costs.

In the present work, a control-oriented energy model of a system of FCUs is developed and accompanied by its identification methodology. The presented methodology consolidates the advantages of physical modelling, identification methods and manufacturer's catalogue data making it robust, simple and easily replicable. Cost-effectiveness of the methodology is reflected in the number of required sensors, e.g. single temperature sensor per each FCU, calorimeters installed only on major supply ducts and temperature sensors in every zone, thus minimizing the commissioning cost for the deployment.

The paper is organized as follows. In Section II, an overview of a control-oriented energy model for a system of FCUs is given. In Section III, an algorithm for finding flow distribution in heating/cooling installations, based on electric-hydraulic analogy is developed. A general thermodynamic model of a FCU is introduced in Section IV. The methodology for identification of the energy model is given in Section V. The test-site configuration is described in Section VI. In Section VII, the developed energy model is experimentally validated on a system of FCUs in the test-site. Section VIII concludes the paper.

II. A CONTROL-ORIENTED ENERGY MODEL FOR A SYSTEM OF FCUS

Control-oriented energy model for a system of FCUs consists of a hydraulic model of the system and thermodynamic models of all FCUs, where thermodynamic model is the same for equal FCU types. The overall scheme of the model is given in Fig. 1. The model inputs are: *i*) central measurement of medium mass flow through the entire system $q^{\mathrm{m}}_{\mathrm{w,o}}$, *ii*) individual measurements of fan speeds x^{m}_i, *iii*) zone air temperatures of every considered zone $T^{\mathrm{in,m}}_{\mathrm{a},i}$ and *iv*) central or individual measurements of supply medium temperature $T^{\mathrm{in,m}}_{\mathrm{w},i}$. Index i in subscripts denotes measurements related to the i^{th} FCU and n is the overall number of FCUs in the system. Outputs of the hydraulic system model are individual medium mass flows through every FCU in the system $q_{\mathrm{w},i}$. Individual medium

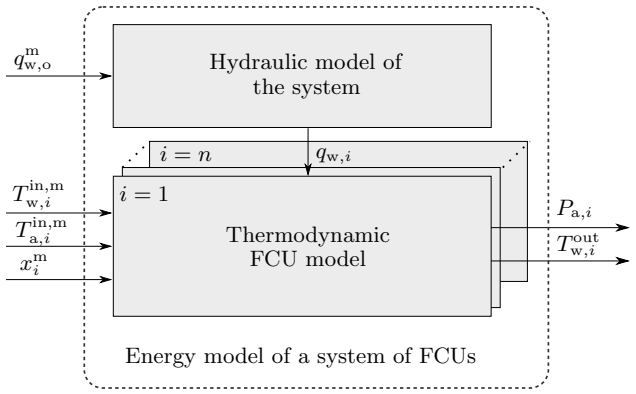

Fig. 1: Scheme of the control-oriented energy model of a system of FCUs.

mass flows are subsequently used in the the thermodynamic models to calculate the thermal powers affecting the zones $P_{\mathrm{a},i}$ and simulated return medium temperatures $T^{\mathrm{out}}_{\mathrm{w},i}$ for every considered FCU.

The developed energy model gives a direct relation between the thermal energy exerted to zone, actuation commands and zone temperature. As such, the model is suitable for: *i*) acquiring thermal powers per zone required for identification of building thermodynamic model, *ii*) estimation of unmeasured thermal loads affecting the zone for a very broad use in building monitoring and control, *iii*) usage of an advanced FCU control algorithm for direct control of thermal energy inputs per zone via fan speeds, which makes it possible to realize optimized thermal energy inputs computed via predictive energy management schemes for maintaining zones thermal comfort [35], [36] and *iv*) development of fault detection and diagnosis algorithms for FCUs [37]–[39].

III. Hydraulic model of a system of FCUs

The medium flow through a FCU depends on the pressure drop across the various elements that form up the entire system. A practical way of modelling complex hydraulic systems is the transition to an analogous electrical model where medium mass flow q_{w}, pressure drop Δp and hydraulic resistance R behave equivalently to electrical current, voltage and electrical resistance, respectively. The equation relating pressure drop and mass flow through a hydraulic network element is equal to:

$$\Delta p = R \cdot q_{\mathrm{w}}^{\alpha}, \tag{1}$$

where R is a constant hydraulic resistance. The values of α depend on the methodology used for calculation of R and the element type.

Pressure loss in pipes consists of three components: *i*) hydrostatic pressure loss Δp_h, *ii*) frictional pressure loss Δp_f and *iii*) kinetic pressure loss. For most applications, kinetic losses are minimal and can be ignored. Thus, the equation that describes the overall pressure loss in pipes is expressed as a sum of two major terms:

$$\Delta p_p = \Delta p_f + \Delta p_h. \tag{2}$$

The hydrostatic pressure drop occurs only when there are differences in elevation from the inlet to the outlet of a pipe segment:

$$\Delta p_h = \rho \cdot g \cdot \Delta h, \tag{3}$$

where g is acceleration of gravity and Δh is change in pipe elevation. The frictional pressure drop in a circular pipe with constant inner diameter d and length l is defined by Darcy-Weisbach equation:

$$\Delta p_f = f_D \frac{8 \cdot l}{\rho \cdot \pi^2 \cdot d^5} \cdot q_{\mathrm{w}}^2, \tag{4}$$

where ρ is the density of heating/cooling medium and f_D is the friction factor. For hydraulically smooth pipes, f_D is defined by Blasius equation:

$$f_D = 0.3164 \cdot Re^{-0.25}, \tag{5}$$

where Re is Reynolds number defined as:

$$Re = \frac{4}{\mu \cdot d \cdot \pi} \cdot q_{\mathrm{w}}, \tag{6}$$

with μ as dynamic viscosity of the medium. In addition to the losses due to the friction or elevation difference, there are also losses associated with flow through valves and fittings. These, so called minor pressure losses, are accounted by using the equivalent length method [40]. The method uses empirical tables to convert each fitting into an equivalent length of the straight pipe l_{eq} which is then added to the pipe length l. The l_{eq}/d ratio for most common types of fittings can be found in [40], [41]. By inserting (6) and (5) into (4) and including the minor losses, the final form of frictional pressure drop across the circular pipe section is defined as:

$$\Delta p_f = 0.241 \cdot \frac{\mu^{0.25} \cdot (l + \sum l_{\mathrm{eq}})}{d^{4.75} \cdot \rho} \cdot q_{\mathrm{w}}^{1.75}. \tag{7}$$

Hydraulic resistance of the FCU and medium mass flow through the unit are fully determined with the pressure drop within it:

$$\Delta p_{\mathrm{fc}} = R_{\mathrm{fc}} \cdot q_{\mathrm{w}}^{\alpha_{\mathrm{fc}}}, \tag{8}$$

where R_{fc} and α_{fc} are parameters to be found based on the experiments or pressure drop data from the manufacturer's catalogue.

Based on the electric-hydraulic analogy an equivalent electrical model of the system is derived for a most common heating/cooling network topology (Fig. 2). Supply pipe, return pipe and FCU hydraulic resistances are denoted as $R^{\mathrm{s}}_{\mathrm{p}}$, $R^{\mathrm{r}}_{\mathrm{p}}$ and R_{fc}, respectively. For clarity, hydraulic resistances of pipes in parallel branches are omitted. For every closed loop of the circuit, once the hydraulic resistances and mass flows are known, the pressure drop is defined with Kirchhoff's circuit laws $\forall j = 1, \ldots, n-1$:

$$\Delta p_j = \begin{cases} \Delta p_{j+1} - \sum_{i=1}^{j} q_{\mathrm{w},i}^{1.75} (R^{\mathrm{s}}_{\mathrm{p},j} + R^{\mathrm{r}}_{\mathrm{p},j}) \text{ for } j \leq k, \\ \Delta p_{j+1} + \sum_{i=j}^{n} q_{\mathrm{w},i}^{1.75} (R^{\mathrm{s}}_{\mathrm{p},j} + R^{\mathrm{r}}_{\mathrm{p},j}) \text{ for } j > k, \end{cases} \tag{9}$$

where Δp_j is the overall pressure drop in a parallel branch including pressure drop through FCU and pressure drop in

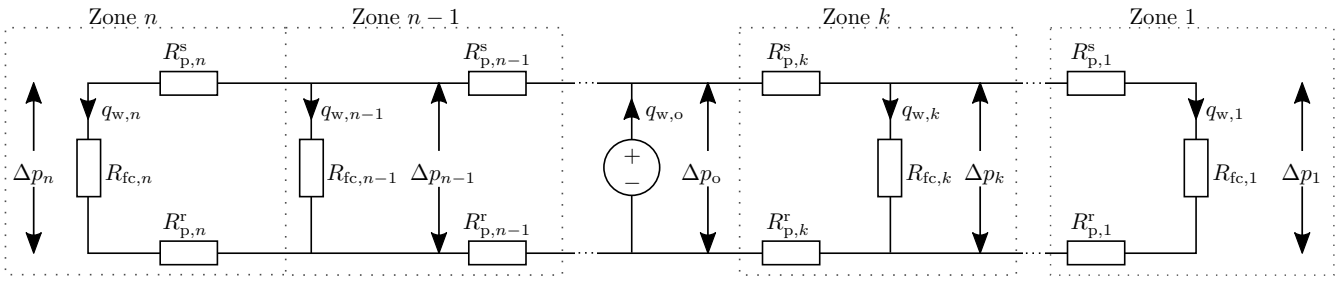

Fig. 2: The analogous electrical model of standard heating/cooling installations.

associated vertical supply and return pipes, $\Delta p_{k+1} = \Delta p_{\mathrm{o}}$ is the overall pressure drop in the entire system, n is the total number of FCUs in the system and $q_{\mathrm{w},i}$ is the medium mass flow though the i^{th} FCU. For known overall medium mass flow denoted with $q^{\mathrm{m}}_{\mathrm{w,o}}$, the individual FCU mass flows $q_{\mathrm{w},i}$ are found by solving the following optimization problem:

$$\begin{aligned} \min_{\Delta p_0} \quad & |q^{\mathrm{m}}_{\mathrm{w,o}} - q_{\mathrm{w,o}}| \\ \text{s.t.} \quad & q_{\mathrm{w,o}} = \sum_{i=1}^{n} q_{\mathrm{w},i}, \\ & (2), (3), (7), (8), (9). \end{aligned} \tag{10}$$

The optimization problem (10) belongs to a class of NonLinear Programs (NLPs) which can be efficiently solved with e.g. genetic algorithms [42]. Flow share through the i^{th} FCU is defined as $\eta_i = q_{\mathrm{w},i}/q_{\mathrm{w,o}}$ where $q_{\mathrm{w},i}$ is recalculated based on (9) and the optimal Δp_0 obtained as solution of optimization problem (10). For installations with operable valves, where flow distribution is time-variable and based on the valve positions, the procedure is extended by introducing variable valves hydraulic resistances in the network.

IV. Thermodynamic FCU model

Heat transfer within a FCU consists of three parts: convection of the heating/cooling medium (e.g. water), heat conduction through the heat exchanger and convection of air to be heated or cooled. For modelling, the following assumptions are made:

- there are four possible fan speeds: off, Low, Medium and High denoted respectively as off, L, M, H,
- air mass flow q_{a} inside the FCU varies with the fan speed and is assumed to be constant for each speed,
- mean water temperature inside the FCU, $\overline{T_{\mathrm{w}}}$, is approximately the average of water inlet temperature $T^{\mathrm{in}}_{\mathrm{w}}$ and water outlet temperature $T^{\mathrm{out}}_{\mathrm{w}}$, i.e. $\overline{T_{\mathrm{w}}} = 0.5(T^{\mathrm{in}}_{\mathrm{w}} + T^{\mathrm{out}}_{\mathrm{w}})$,
- heat transfer from water to air is driven by the temperature difference $(\overline{T_{\mathrm{w}}} - T^{\mathrm{in}}_{\mathrm{a}})$,
- air intake temperature $T^{\mathrm{in}}_{\mathrm{a}}$ is assumed to be equal to zone temperature,
- properties of air and water are assumed to be constant.

With set assumptions, the following dynamics equations are derived for each FCU:

$$m_{\mathrm{w}} c_{\mathrm{w}} \dot{T}^{\mathrm{out}}_{\mathrm{w}} = q_{\mathrm{w}} c_{\mathrm{w}} (T^{\mathrm{in}}_{\mathrm{w}} - T^{\mathrm{out}}_{\mathrm{w}}) - U_{\mathrm{o}} \left(\overline{T_{\mathrm{w}}} - T^{\mathrm{in}}_{\mathrm{a}}\right), \tag{11}$$

$$m_{\mathrm{a}} c_{\mathrm{a}} \dot{T}^{\mathrm{out}}_{\mathrm{a}} = q_{\mathrm{a}} c_{\mathrm{a}} (T^{\mathrm{in}}_{\mathrm{a}} - T^{\mathrm{out}}_{\mathrm{a}}) + U_{\mathrm{o}} \left(\overline{T_{\mathrm{w}}} - T^{\mathrm{in}}_{\mathrm{a}}\right), \tag{12}$$

where $T^{\mathrm{out}}_{\mathrm{a}}$ is the outgoing air temperature, q_{w} is medium mass flow through the FCU, c_{a} and c_{w} are the specific heat capacity of dry air and specific heat capacity of water, respectively. Parameter m_{a} is the mass of air and m_{w} is the mass of water inside the FCU, available from manufacturer's catalogue. Heat transfer coefficient $U_{\mathrm{o}} = f(q_{\mathrm{a}}, q_{\mathrm{w}})$ is a nonlinear function of medium mass flow q_{w} and airflow q_{a} defined as [34], [38], [43]:

$$U_{\mathrm{o}}(q_{\mathrm{a}}, q_{\mathrm{w}}) = \frac{a \cdot q_{\mathrm{a}}^{\beta}}{1 + b \cdot \left(\dfrac{q_{\mathrm{a}}}{q_{\mathrm{w}}}\right)^{\beta}}, \tag{13}$$

where a, b and β are parameters determined based on physical system properties or through identification. For FCUs with fixed set of fan speeds, the air mass flow q_{a} for a certain fan speed x does not deviate over time significantly (if there are no external impacts blocking the air path). Thus, it is reasonable to estimate separate functional dependencies for all available fan speeds avoiding thus the need for knowing the exact, hardly measurable, information on the airflow. By linking the airflow information to a fan speed, (13) obtains the form:

$$U_{\mathrm{o}}(x, q_{\mathrm{w}}) = \begin{cases} \dfrac{a^{\mathrm{off}}}{1 + b^{\mathrm{off}} \cdot q_{\mathrm{w}}^{-\beta}}, & \text{for} \quad x = \text{off}, \\ \dfrac{a^{\mathrm{L}}}{1 + b^{\mathrm{L}} \cdot q_{\mathrm{w}}^{-\beta}}, & \text{for} \quad x = \mathrm{L}, \\ \dfrac{a^{\mathrm{M}}}{1 + b^{\mathrm{M}} \cdot q_{\mathrm{w}}^{-\beta}}, & \text{for} \quad x = \mathrm{M}, \\ \dfrac{a^{\mathrm{H}}}{1 + b^{\mathrm{H}} \cdot q_{\mathrm{w}}^{-\beta}}, & \text{for} \quad x = \mathrm{H}, \end{cases} \tag{14}$$

with individual parameters $\mathbf{a} := \{a^{\mathrm{off}}, a^{\mathrm{L}}, a^{\mathrm{M}}, a^{\mathrm{H}}\}$ and $\mathbf{b} := \{b^{\mathrm{off}}, b^{\mathrm{L}}, b^{\mathrm{M}}, b^{\mathrm{H}}\}$ defined for every fan speed. Parameter β does not depend on the airflow so one common parameter for all fan states is defined. For switched-off fan a FCU behaves as a normal radiator unit with a constant heat transfer coefficient, thus for fan switched off $b^{\mathrm{off}} = 0$.

The thermodynamic performance of the floor mounted units is downgraded during the cooling season. While during the heating season, incoming air temperature is considered equal to the zone temperature, during the cooling season cooled outgoing air tends to settle at the floor without mixing with the zone air. As a result, incoming air temperatures are lower than the zone temperature. The described seasonal effect is

anticipated through introduction of correction coefficients ε^x for every fan speed:

$$U_{\mathrm{o}}(x, q_{\mathrm{w}}) = \varepsilon^x \cdot \frac{a^x}{1 + a^x \cdot q_{\mathrm{w}}^{-\beta}}, \quad x \in \{\text{off, L, M, H}\}. \quad (15)$$

The m_a/q_a ratio is typically less than 1 s and therefore negligible compared to water time constant. The air side thermal process of a FCU is therefore observed as a stationary process ($\dot{T}_{\mathrm{a}}^{\mathrm{out}} = 0$):

$$\underbrace{q_{\mathrm{a}} c_{\mathrm{a}} (T_{\mathrm{a}}^{\mathrm{out}} - T_{\mathrm{a}}^{\mathrm{in}})}_{P_a} = \underbrace{U_{\mathrm{o}} \left(\overline{T_{\mathrm{w}}} - T_{\mathrm{a}}^{\mathrm{in}}\right)}_{P_t}. \quad (16)$$

This further means that the thermal power affecting the zone, P_a, is equal to the overall transmitted thermal power P_t. The important feature of this approach is that the hardly measurable and unreliable $T_{\mathrm{a}}^{\mathrm{out}}$ measurement is omitted. For a fixed medium mass flow q_{w}, the final thermodynamic model of a FCU is in a form of a switched-linear model:

$$\begin{aligned} \dot{T}_{\mathrm{w}}^{\mathrm{out}} = &\left[-\frac{q_{\mathrm{w}}}{m_{\mathrm{w}}} - \frac{U_{\mathrm{o}}(x, q_{\mathrm{w}})}{2 m_{\mathrm{w}} c_{\mathrm{w}}} \right] T_{\mathrm{w}}^{\mathrm{out}} \\ &+ \begin{bmatrix} \frac{q_{\mathrm{w}}}{m_{\mathrm{w}}} - \frac{U_{\mathrm{o}}(x, q_{\mathrm{w}})}{2 m_{\mathrm{w}} c_{\mathrm{w}}} & \frac{U_{\mathrm{o}}(x, q_{\mathrm{w}})}{m_{\mathrm{w}} c_{\mathrm{w}}} \end{bmatrix} \begin{bmatrix} T_{\mathrm{w}}^{\mathrm{in}} \\ T_{\mathrm{a}}^{\mathrm{in}} \end{bmatrix}, \end{aligned} \quad (17)$$

$$\begin{aligned} P_{\mathrm{a}} = &\left[\frac{U_{\mathrm{o}}(x, q_{\mathrm{w}})}{2} \right] T_{\mathrm{w}}^{\mathrm{out}} \\ &+ \begin{bmatrix} \frac{U_{\mathrm{o}}(x, q_{\mathrm{w}})}{2} & -U_{\mathrm{o}}(x, q_{\mathrm{w}}) \end{bmatrix} \begin{bmatrix} T_{\mathrm{w}}^{\mathrm{in}} \\ T_{\mathrm{a}}^{\mathrm{in}} \end{bmatrix}, \end{aligned} \quad (18)$$

where $U_{\mathrm{o}}(x, q_{\mathrm{w}})$ is defined in (14) and the fan speed x is used for switching.

V. The identification methodology

The methodology for identification of an energy-model of a system of FCUs consists of three major parts: *i*) sensors calibration, *ii*) identification of a hydraulic system model, and *iii*) identification of thermodynamic FCUs models. The considered system configuration consists of: *i*) multiple FCUs connected in parallel, *ii*) temperature sensors installed on the FCU return pipes measuring the return medium temperature, *iii*) zone units for measuring the zone air temperature and fan speed, and *iv*) central calorimeter for measuring the overall medium mass flow through the system, supply and return medium temperatures and thermal consumption of the entire system. Supply and return pipes are assumed to be isolated. All measurements are collected with a time resolution of T_s.

A. Sensors calibration

Indirect measurement of the return medium temperature, typically performed with temperature sensor mounted on the FCU return pipe is subject to various effects (e.g. lead wires acting as a thermal sink, sensor insulation, effects of ambient temperature, etc.) that cause its deviation from the real temperature. The so-called two-point calibration method, comparison with trusted sensor at lower and upper bound of the operating range, essentially re-scales the output and is capable of correcting both slope and offset errors. For systems with three-way valves (Fig. 3) and well-insulated

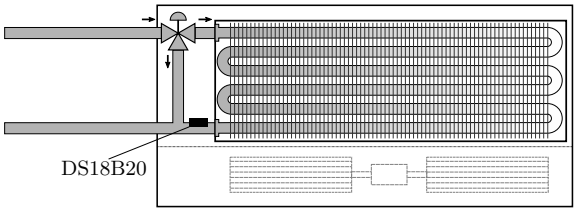

Fig. 3: FCU installation with three-way valve and 1-wire return medium temperature sensor (DS18B20) mounted on the return pipe.

supply pipelines, the sensor characteristics can be determined by using historical measurements. In intervals with switched off fan and closed FCU valve (total flow goes through the bypass branch), calibrated sensor measurements should be equal to measurements of supply temperature T_{cal}. The sensor calibration curve, defined with slope $p_{1,i}$ and offset $p_{2,i}$, is then found by solving the following optimization problem:

$$\min_{p_{1,i}, p_{2,i}} \quad \sum_{k=1}^{M_i} \left(T_{\mathrm{w},i}^{\mathrm{out,c}}(k) - T_{\mathrm{cal}}^{\mathrm{m}}(k) \right)^2, \quad (19)$$

where k denotes measurement samples, M_i is overall number of samples used for calibration, $T_{\mathrm{w},i}^{\mathrm{out,c}} = p_{1,i} T_{\mathrm{w},i}^{\mathrm{out,raw}} + p_{2,i}$ is the calibrated sensor measurement and $T_{\mathrm{w},i}^{\mathrm{out,raw}}$ is a raw sensor measurement of the i^{th} FCU. If temperature sensor is mounted close to the bypass branch, measurements may be additionally distorted due to the high thermal conductivity of the pipes. Since supply and return pipes are thermally coupled through the bypass, large thermal gradient between them influences the sensor measurements proportionally to temperature difference between the pipes. True temperature measurement $T_{\mathrm{w},i}^{\mathrm{out,m}}$ is thus defined as:

$$T_{\mathrm{w},i}^{\mathrm{out,m}} = T_{\mathrm{w},i}^{\mathrm{out,c}} - \phi (T_{\mathrm{w},i}^{\mathrm{in,m}} - T_{\mathrm{w},i}^{\mathrm{out,m}}), \quad (20)$$

where ϕ is the unknown heat transfer coefficient equal for all FCUs with the same bypass pipe configuration and $T_{\mathrm{w},i}^{\mathrm{in,m}}$ is the ith FCU supply temperature considered equal to $T_{\mathrm{cal}}^{\mathrm{m}}$. For ideal mixing of the return medium from different FCUs and only the i^{th} FCU operating at the time (valves on all other FCUs closed) once stationary state is reached, the following holds:

$$q_{\mathrm{w},i} (T_{\mathrm{w},i}^{\mathrm{in}} - T_{\mathrm{w},i}^{\mathrm{out}}) = q_{\mathrm{w,o}} (\Delta T_{\mathrm{cal},i} - \Delta T_{\mathrm{cal},0}). \quad (21)$$

where $\Delta T_{\mathrm{cal},i}$ is temperature difference between the system supply and return measured on the central calorimeter and $\Delta T_{\mathrm{cal},0}$ is the temperature difference in the system with valves of all FCUs closed. Since $\sum_{i=1}^{n} q_{\mathrm{w},i} = q_{\mathrm{w,o}}$, by combining (20) and (21) heat transfer coefficient ϕ is defined as:

$$\phi = 1 - 1 \Big/ \sum_{i=1}^{n} \left(\frac{\Delta T_{\mathrm{cal},i} - \Delta T_{\mathrm{cal},0}}{T_{\mathrm{w},i}^{\mathrm{in}} - T_{\mathrm{w},i}^{\mathrm{out,c}}} \right), \quad (22)$$

where n is the total number of FCUs in the system.

B. Identification of the hydraulic system model

The prerequisites for development of an analogous electrical model of the heating/cooling system are *i*) the availability

of system documentation with known diameters and lengths of individual pipe segments and *ii*) FCUs manufacturers' catalogues with specified pressure drop characteristics. Based on the developed analogous electrical model, the flow shares through different FCUs are defined by the solution of optimization problem (10). If the pressure drop at the system entrance is changed, new flow distribution is found by re-solving (10) based on new measurement of overall flow through the system $q^{\mathrm{m}}_{\mathrm{w,o}}$.

If the piping data or FCUs pressure drop characteristics are not available, the approach based on running an individual experiment on every FCU is proposed. It is important to note that so obtained flow distribution is valid only for operating points for which the experiments are performed. If the overall pressure drop of the system is changed, experiments have to be performed again under new conditions. Thus, the approach is not advisable for systems with variable flow. Since such approach is time consuming for large systems, herein it is used for validation of the approach based on electric-hydraulic analogy. The individual experiments are performed by switching off all the units in the system (or assuring their constant operation) and running a test sequence on one particular unit. Valves remained fully opened for all units. In such a set-up, the central calorimeter measures the heat consumption of the particular unit with a constant offset equal to the thermal power of the remaining part of the system. To assure constant losses, supply medium mass flow and temperature are required to be constant during the test. The test sequence consists of switching on the highest fan speed on the i^{th} unit and keeping it on until the stationary state is reached. The hydronic systems are inevitably subject to transport delays. To account for the effect, calorimeter and return medium temperature measurements are considered as ideal with variable transport delay τ estimated based on the known pipe length and diameter as well as the medium mass flow. After performing experiments on every FCU, flow share through the i^{th} unit η_i is found by solving the following optimization problem:

$$\begin{aligned} \min_{\eta_i, P_d} \quad & \sum_{k=1}^{M_i} \left(\eta_i \cdot P^{\mathrm{a}}_{\mathrm{w},i}(k) - (P^{\mathrm{m}}_{\mathrm{cal}}(k+\tau_{\mathrm{cal}}) - P_{\mathrm{d}})\right)^2 \\ s.t. \quad & P^{\mathrm{a}}_{\mathrm{w},i}(k) = q^{\mathrm{m}}_{\mathrm{w,o}}(k) c_{\mathrm{w,cal}} \left(T^{\mathrm{in,m}}_{\mathrm{w},i}(k) - T^{\mathrm{out,m}}_{\mathrm{w},i}(k+\tau_{\mathrm{fc}})\right), \\ & 0 \le \eta_i \le 1, \end{aligned} \tag{23}$$

where k denotes measurement samples, M_i is the overall number of the samples in the experiment with the i^{th} FCU, $c_{\mathrm{w,cal}}$ is a nominal water heat capacity used by the calorimeter (usually set to heat capacity of distilled water $c_{\mathrm{dw}} = 4180$ J/(kgK)), $P^{\mathrm{m}}_{\mathrm{cal}}$ is thermal power measurement from the calorimeter, $P^{\mathrm{a}}_{\mathrm{w},i}$ is a-priori water-side thermal power of the i^{th} FCU and P_{d} is constant thermal power consumed by the rest of the system. For clarity, the transport delay τ_{fc} is assumed to be already accounted when using the return medium temperature measurements in the rest of the paper.

For available measurement of the system return medium temperature $T^{\mathrm{out,m}}_{\mathrm{w,cal}}$ and medium mass flow and supply temperature constant during the experiment, simple algebraic equations for calculation of flow share through the i^{th} FCU are derived. Flow share of the i^{th} FCU is defined as the ratio of temperature differences of the system and FCU return temperature with all FCUs' fans switched off (denoted with superscript 'off') and measured once stationary state of return medium temperature of the excited unit is reached (denoted with superscript 'on'):

$$\eta_i = \left| \frac{(T^{\mathrm{out,m,off}}_{\mathrm{w,cal}} - T^{\mathrm{out,m,on}}_{\mathrm{w,cal}})}{(T^{\mathrm{out,m,off}}_{\mathrm{w},i} - T^{\mathrm{out,m,on}}_{\mathrm{w},i})} \right|. \tag{24}$$

C. Identification of a thermodynamic FCU model

In the majority of water-based heating and cooling systems, medium mass flow is controlled to a constant value while supply temperature is altered to meet the building thermal demand. Thus, from the operation data of one FCU only the number of points on the $U_{\mathrm{o}} = f(x, q_{\mathrm{w}})$ characteristics equal to the number of available distinct fan speeds can be obtained. To obtain multiple points for different medium mass flows the non-uniform distribution of the flow through the system is exploited, i.e. several FCUs of the same type with different estimated flow shares are examined. For a fixed medium mass flow and fan speed, overall heat transfer coefficient is a scalar value (14). The identification of the U_{o} characteristic is thus divided into two parts. First, a set of scalars $\mathbf{U}_{\mathrm{o}} = \{U^{\mathrm{off}}_{\mathrm{o}}, U^{\mathrm{L}}_{\mathrm{o}}, U^{\mathrm{M}}_{\mathrm{o}}, U^{\mathrm{H}}_{\mathrm{o}}\}$ is found by solving the following optimization problem for every dataset related to the considered FCUs of the same type:

$$\begin{aligned} \min_{\mathbf{U}_{\mathrm{o}}, c_w} \quad & \sum_{k=1}^{M_i} |T^{\mathrm{out,m}}_{\mathrm{w},i}(k) - T^{\mathrm{out}}_{\mathrm{w},i}(k)| \\ \text{s.t.} \quad & q_{\mathrm{w},i}(k) = \eta_i \cdot q^{\mathrm{m}}_{\mathrm{w,o}}(k), \\ & (14). \end{aligned} \tag{25}$$

Index k denotes measurement samples, c_{w} is unknown water heat capacity, $T^{\mathrm{out,m}}_{\mathrm{w},i}$ is measured return medium temperature of the i^{th} FCU and M_i is the length of the considered data set. The output of the thermodynamic FCU model $T^{\mathrm{out}}_{\mathrm{w},i}(k)$ is defined as:

$$T^{\mathrm{out}}_{\mathrm{w},i}(k+1) = h\left(x^{\mathrm{m}}_i(k), q_{\mathrm{w},i}(k), T^{\mathrm{in,m}}_{\mathrm{w},i}(k), T^{\mathrm{in,m}}_{\mathrm{a},i}(k), T^{\mathrm{out}}_{\mathrm{w},i}(k)\right), \tag{26}$$

with function $h(\cdot)$ representing numerical integration of (17) over the interval $[k, k+1]T_s$ and model inputs assumed to be constant within that interval. For systems with known heat capacity of the medium c_{w} operating in a stationary state, values of the $\mathbf{U}_{\mathrm{o}}$ set for a fixed medium mass flow $q_{\mathrm{w},i}$ and fan speed x_i are defined as:

$$U^x_{\mathrm{o}} = \frac{q_{\mathrm{w},i} c_{\mathrm{w}} (T^{\mathrm{in,m}}_{\mathrm{w},i} - T^{\mathrm{out,m},x}_{\mathrm{w},i})}{(0.5 \cdot (T^{\mathrm{in,m}}_{\mathrm{w},i} + T^{\mathrm{out,m},x}_{\mathrm{w},i}) - T^{\mathrm{in,m}}_{\mathrm{a},i})}. \tag{27}$$

The result of the first part of the thermodynamic model identification is a set of value triplets $\{(q^*_{\mathrm{w},i}, x^*_i, U^{x*}_{\mathrm{o}})_j : j = 1, ..., K\}$, where K is their overall number and $q^*_{\mathrm{w},i}$ is mean value of the medium mass flow of the considered data set if the triplets are obtained by solving (25) or it is equal to medium mass flow used in (27).

The second part of the identification is related to finding the unknown coefficients of the U_o characteristics (15). The unknown coefficients are found by minimizing the squared error between the model (15) and value triplets obtained experimentally:

$$\min_{\mathbf{a},\mathbf{b},\boldsymbol{\varepsilon},\beta} \quad \sum_{j=1}^{K} (U_\mathrm{o}(x_i^*, q_{\mathrm{w},i}^*) - U_\mathrm{o}^{x*})^2, \tag{28}$$

where $\boldsymbol{\varepsilon}$ is a set off FCU efficiencies in every fan speed $\boldsymbol{\varepsilon} := \{\varepsilon^{\mathrm{off}}, \varepsilon^{\mathrm{L}}, \varepsilon^{\mathrm{M}}, \varepsilon^{\mathrm{H}}\}$ and $U_\mathrm{o}(x_i^*, q_{\mathrm{w},i}^*)$ is defined as in (15). To improve the performance of the model outside the current operating range of the system additional value pairs are calculated form the catalogue data based on the stationary equation (16).

Following from (14), it is evident that heat transfer coefficient U_o increases with the medium mass flow q_w. However, due to distinctively higher heat capacity of the medium compared to air, for fixed fan speed the U_o value starts to stagnate after some amount of medium mass flow:

$$\lim_{q_\mathrm{w}\to\infty} U_\mathrm{o}(x, q_\mathrm{w}) = a^x, \quad x \in \{\text{off, L, M, H}\}. \tag{29}$$

This part of the U_o characteristics is typically covered in manufacturer's catalogue. The heat capacity tables from the catalogue consist of stationary values of the sensible thermal power data $P_\mathrm{a}^{\mathrm{cd}}$, supply $T_\mathrm{w}^{\mathrm{in,cd}}$ and return $T_\mathrm{w}^{\mathrm{out,cd}}$ temperature of the heating/cooling medium and entering air temperature data $T_\mathrm{a}^{\mathrm{in,cd}}$ for different fan speeds. Thus, if such data are available it is possible to calculate values in the **a** coefficient set from the stationary condition (16) as:

$$a^x = \left| \frac{P_\mathrm{a}^{\mathrm{cd,x}}}{\left(T_\mathrm{a}^{\mathrm{in,cd,x}} - 0.5\left(T_\mathrm{w}^{\mathrm{in,cd,x}} + T_\mathrm{w}^{\mathrm{out,cd,x}}\right)\right)} \right|. \tag{30}$$

It is important to note that, even without the use of the manufacturer's catalogue data, it is possible to estimate the model covering the operating range of the system. Since the catalogue data cover the constant part of the U_o characteristics, it represents a sort of performance bound for the considered FCUs.

General-purpose compact identification methods are unable to cope with the problem of identifying the presented energy model due to the multiple local minima occurring as a result of a large number of unknown parameters and high nonlinearity of the model (14). The problem is avoided by breaking the procedure into several parts, the workflow of which is given in Fig. 4. The optimization problems (19) and (23) are in a form of a Quadratic Program (QP), efficiently solved by using QP or any generic NLP optimization solver in MATLAB. The optimization problems (25) and (28) belong to a class of NLPs and are efficiently solved by using e.g. Levenberg-Marquardt algorithm in MATLAB [42].

VI. Test-site configuration

The considered living-lab at University of Zagreb Faculty of Electrical Engineering and Computing spans over 12 floors of the university skyscraper. The building has east-west orientation with overall 248 controllable zones. Each floor in

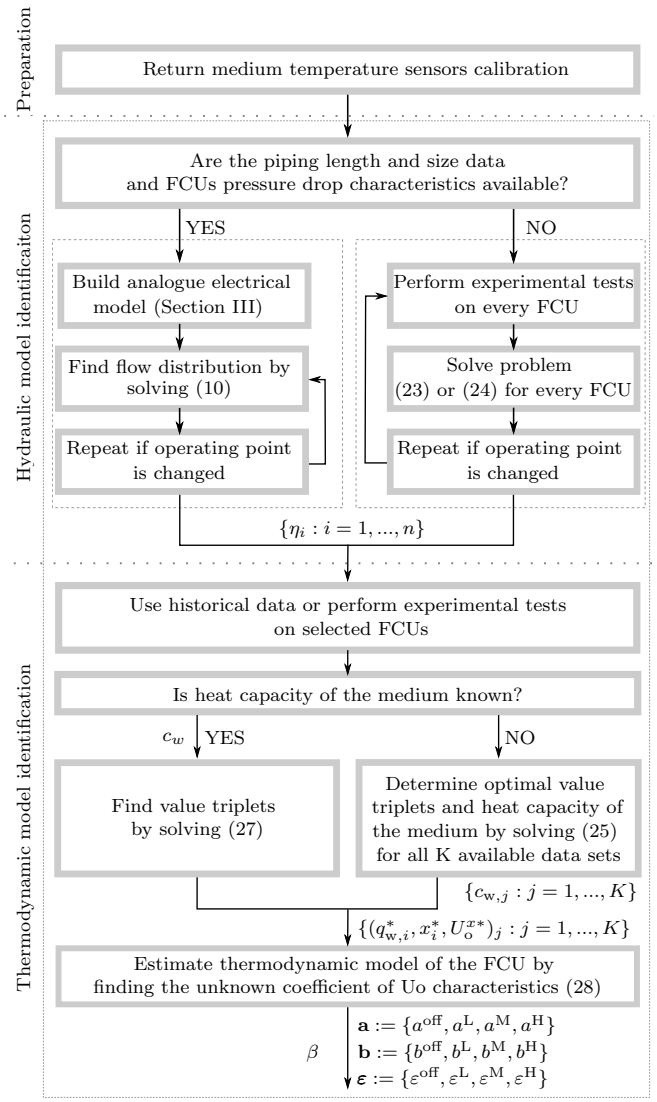

Fig. 4: The workflow of the methodology for identification of an energy model for a system of FCUs.

the building has separate north-side and south-side piping and thus a separate north-side and south-side FCU system as considered in this paper. The central part of the living lab is a database with data acquisition operating on a minute timescale. The two-pipe system is used for seasonal heating and cooling. The FCUs, produced by manufacturer Trane (models FCC06 and FCC04) [44], are equipped with a centrifugal fan with four different fan speeds (off, Low, Medium and High). Additionally, FCUs on the 9th and 10th floor are equipped with a three-way valve (on-off type). Both fan speed and valve position are controlled by Siemens RXC21.1/RXC21.5 zone temperature controllers operating on LonWorks network. Each controllable zone includes a separate user interface for temperature reference selection (QAX34.1 device). The existing communication network is enhanced such that the RXC controllers are reconfigured to be able to pass the information to a central database (current zone temperature, fan speed and valve actuation) and to be able to receive the commands from the database (fan speed, valve actuation). All the FCUs in the

same zone are actuated simultaneously. The system is further upgraded with low-cost 1-wire digital temperature sensors DS18B20 installed on the FCUs return pipes (Fig. 3). On two selected FCUs, additional 1-wire sensors are mounted to investigate the effect of downgraded FCU performance during the cooling season and monitor incoming and outgoing air temperatures (Fig. 5).

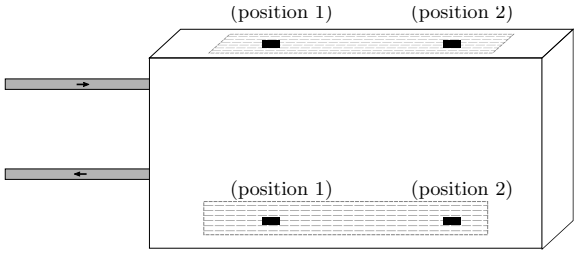

Fig. 5: Placement of additional 1-wire sensors for monitoring incoming and outgoing air temperatures.

Siemens calorimeters UH50-A50-00 operating on M-Bus protocol are installed on every floor supply duct. Calorimeters measure supply and return medium temperature, temperature difference, medium flow, thermal power and consumed thermal energy with one minute time resolution. All the systems are integrated together with a network controller unit employed to enable two-way communication between devices operating on different protocols. Logical organization of the described system is shown in Fig. 6.

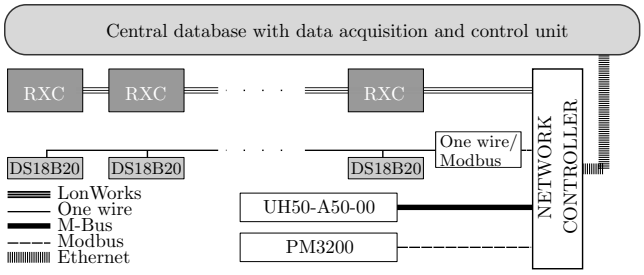

Fig. 6: Logical organization of the living-lab sensor-actuator network.

The article is focused on the FCU system of the south-side piping on the 9th floor consisted of 13 zones with 17 vertical FCUs mounted on the floor, 12 units of type FCC06 and 5 units of type FCC04 (Fig. 7). The arrangement of units with included geometry of supply pipes (length and diameter) is given in columns 2 through 4 in Table I. The length of the pipe is defined as the length of the horizontal segment between two consecutive FCUs or the length between the FCU and the calorimeter (see Fig. 7). The equivalent length of vertical supply and return pipes (including fittings) is identical for all units and amounts $l + \sum l_{\text{eq}} = 6.26$ m. In the following subsections, transmission heat losses are neglected due to the good thermal insulation of the pipeline. This means that the FCU water inlet temperature is considered to be equal to the supply temperature measured by the calorimeter T_{cal} ($T^{\text{in}}_{\text{w},i} = T_{\text{cal}}$). If the temperature drop along the network is significant, it should be modelled or additional temperature sensors have to be mounted at the FCU water inlet.

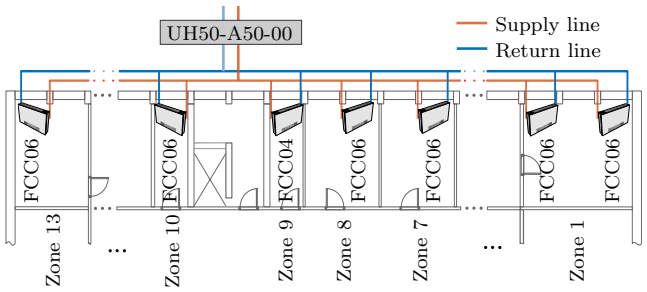

Fig. 7: Layout of the southern supply duct on the 9th floor.

VII. Experimental validation on the test-site

Since validation of both thermodynamic and hydraulic model requires experiments, one common set of experiments per FCU is used. The experiments are performed by shutting down all the units and running a test sequence on one particular unit. Valves remained fully opened for all units. The test sequence consists of sequential fan speed changes from off to other possible fan speeds. The duration of every speed engagement is chosen to be 8 min, which proved to be enough to cover both the transient and steady-state behaviour. Alternatively, the identification of the thermodynamic model is also applicable on FCU historical data with the requirement of recorded stationary operation for each fan speed. Measurements obtained after running the experiment test on the selected Zone 7 during the heating season 2016/17 are shown in Fig. 8.

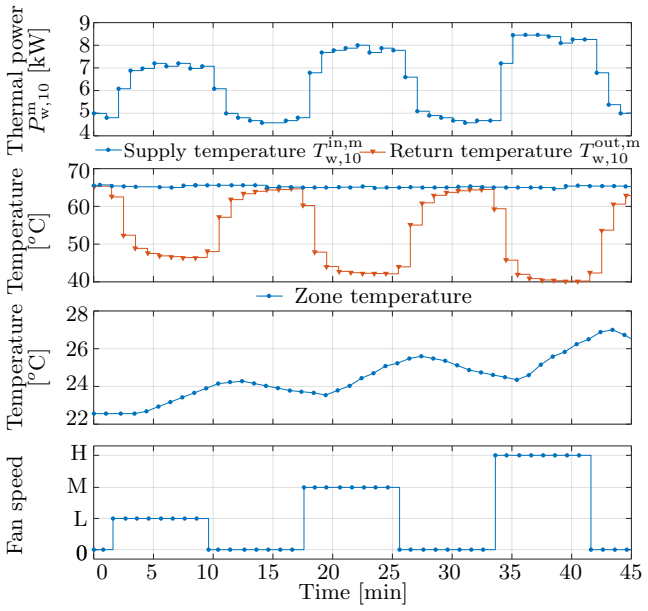

Fig. 8: Measurements obtained after running the experiment test in the exemplary Zone 7 (FCU i=10).

A. 1-wire return medium temperature sensors calibration

Due to the well-insulated supply pipelines, large thermal conductivity of the copper pipes and 1-wire sensor mounted near to the bypass branch, offset characteristics is determined

using historical measurements of supply medium temperature. To avoid the transient impact of the medium stalled inside the heat exchanger, only stationary values are used. Figure 9 shows the calibration curve obtained by calibrating the 1-wire sensor mounted on the FCU return pipe in Zone 7.

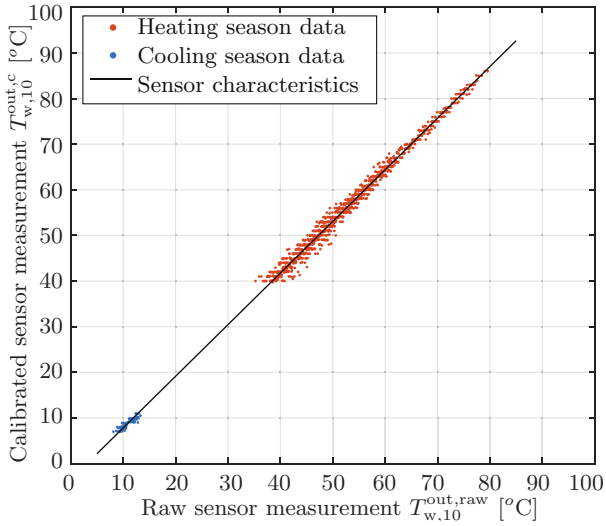

Fig. 9: 1-wire return medium temperature sensor characteristics (FCU $i = 10$).

To determine the coefficient ϕ, the identification procedure according to (22) was performed. The resulting ϕ value for the test-site and described scenario amounts $\phi = 0.1534$.

B. Identification of the hydraulic test-side model

With known topology and geometry of the pipes (see the first four columns in Table I), an analogous electrical model of the test-site hydraulic installations is developed. The correlation between pressure drop and mass flow for both FCU types is found by identifying the unknown coefficients R_{fc} and α_{fc} based on the data from the manufacturer's catalogue (see e.g. Fig. 10 for FCC06 FCU type).

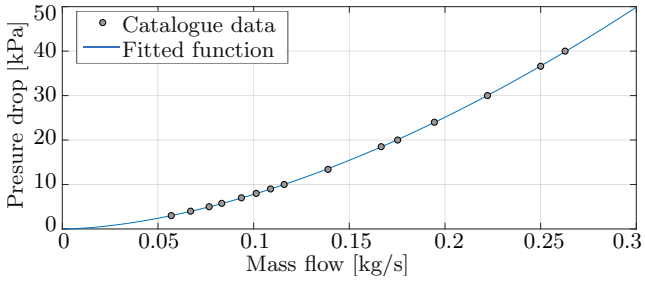

Fig. 10: Identified pressure drop function for Trane model FCC06.

To set up the optimization problem (10), a single measurement of the overall medium mass flow $q_{\text{w,o}}^{\text{m}}$ from the calorimeter is used. The flow distribution through the entire network is found by solving the optimization problem (10) in MATLAB with the genetic algorithm from [42]. The resulting flow distribution, defined as $\eta_i = q_{\text{w,i}}/q_{\text{w,o}}$ and rounded to two decimals, is listed in the sixth column of Table I.

TABLE I: Estimated flow share for the south supply line on the 9th floor for $q_{\text{w,o}}^{\text{m}} \approx 0.36$ kg/s.

Zone No.	FCU No. i	d [mm]	l [m]	Unit type	η_i [%]	$\bar{\eta}_i$ [%]	Error $\frac{\lvert\eta_i - \bar{\eta}_i\rvert}{\eta_i}$ [%]
1	1	18	1.7	FCC06	4.62	4.73	0.04
	2	22	3.5	FCC06	4.85		
2	3	28	1.7	FCC06	5.40	5.49	0.13
	4	35	3.5	FCC06	5.60		
3	5	35	3.5	FCC06	5.81	5.88	1.22
4	6	35	3.5	FCC06	6.09	5.97	1.87
5	7	42	3.5	FCC06	6.49	6.50	0.24
6	8	42	1.7	FCC04	5.31	x	x
	9	42	3.5	FCC04	5.51		
7	10	42	3.5	FCC06	7.20	7.40	2.84
8	11	42	1.7	FCC06	7.58	7.66	1.06
9	12	42	2.1	FCC04	6.01	6.15	2.27
10	13	28	5	FCC06	7.08	x	x
11	14	28	1.7	FCC06	6.77	6.71	0.79
12	15	28	3.5	FCC04	5.00	4.94	1.13
	16	22	1.7	FCC04	4.77		
13	17	18	3.5	FCC06	5.62	x	x

Flow shares, identified based on (23) and individual experiments, for 8 tests performed in the exemplary Zone 7 during winter 2015 and 2016, are shown in Table II.

TABLE II: Estimated flow share for Trane FCC06 based on (23) in Zone 7 (FCU $i = 10$).

Test No.	1	2	3	4	5	6	7	8
$q_{\text{w},10}$ [kg/s]	0.027	0.028	0.027	0.028	0.029	0.023	0.022	0.030
$100 \cdot \eta_{10}$ [%]	7.26	7.35	7.35	7.57	7.34	7.26	7.78	7.31

The mean flow share is $\bar{\eta}_{10} = 7.40\%$, which deviates from the calculated value based on the electric-hydraulic analogy by only 2.84% (see Table I). The identified flow distribution through the test-site is listed in the seventh column of Table I. Since all FCUs in a single zone are actuated simultaneously, for zones with more than one FCU, the mean flow share of all units is calculated instead of individual shares. Average relative error, mainly due to sensor accuracy, is 1.16%, which proves the adequate accuracy of electric-hydraulic analogy based calculation of flow distribution through the system. In zones marked with 'x', measurements were unavailable.

C. Identification of the thermodynamic model of test-site FCUs

Value triplets for identification of the thermodynamic model of the selected FCU type (FCC06) are identified by solving the optimization problem (25) for the data collected during 32 test sequence runs on the units of type FCC06 in different zones during heating season 2015/2016, 2016/2017 and cooling season 2017. The optimization problem is solved by using Levenberg-Marquardt algorithm in MATLAB [42]. The heat capacity of water c_w identified according to (25) for all the experiments is shown in Fig. 11. The model (26) used in optimization (25) is initialized by using the known measurements of the return medium temperature at the beginning of each of the experiments. During the heating season incoming air temperature can be considered equal to the zone temperature,

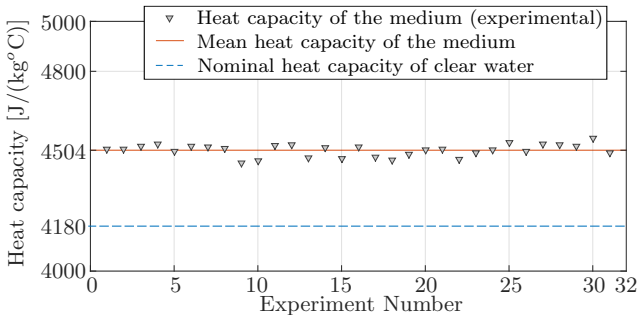

Fig. 11: Identified heat capacity of the heating/cooling medium.

thus ε^x coefficients are set to one for all speeds. During the cooling season cooled outgoing air tends to settle at the floor without mixing with the zone air (Fig. 12).

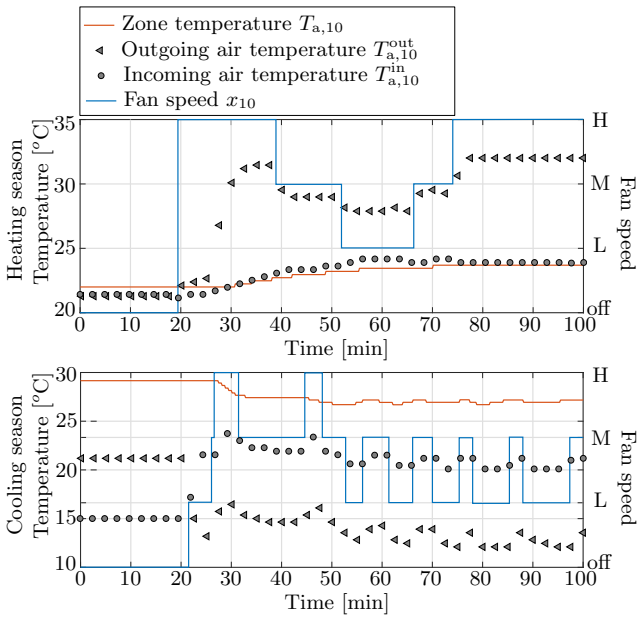

Fig. 12: Measurements of incoming and outgoing air temperature for FCU $i = 10$.

To anticipate the effect, separate efficiency coefficients ε^x are identified for every fan speed, see (15). The identified parameter sets **a**, **b** and $\boldsymbol{\varepsilon}$ and parameter β for Trane FCC06 thermodynamic model obtained through (28), based on the above obtained value triplets, are shown in Table III.

TABLE III: Estimated $U_o(x, q_w)$ function parameters for Trane FCC06.

Fan speed x/ Model parameters	off	L	M	H
a^x	5.30	96.45	152.90	201.80
b^x	0	$1.73{\cdot}10^{-3}$	$3.58{\cdot}10^{-3}$	$5.40{\cdot}10^{-3}$
ε^x (cooling)	0	0.35	0.47	0.52
ε^x (heating)			1	
β			1.86	

Time responses of the identified thermodynamic model for one exemplary zone, tested on the verification data set, are shown in Fig. 13. The model is simulated by using known model input data to calculate the prediction of the return

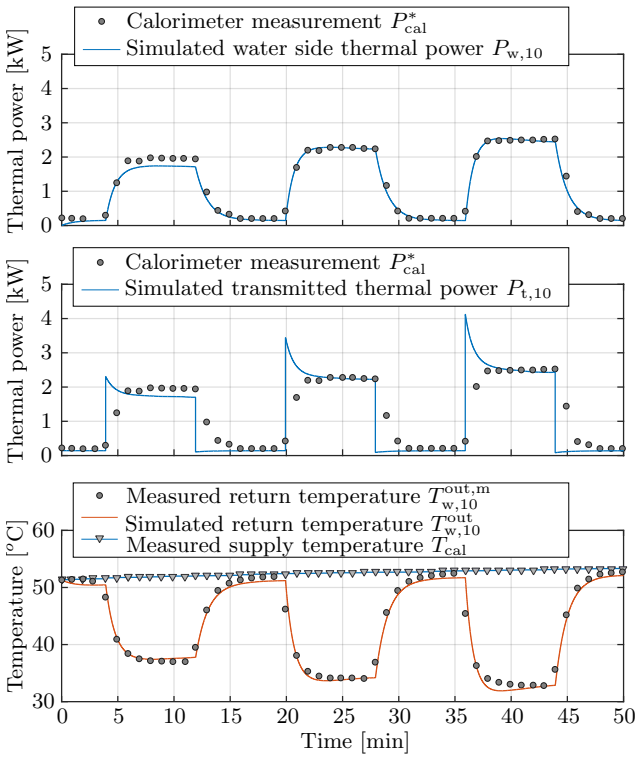

Fig. 13: Identified FCU model (FCU i=10) response over the verification data set.

medium temperature without considering available measurements during that period (so-called open-loop prediction). Estimated heat capacity of the medium is considered (see Fig. 11) such that calorimeter power measurements are scaled and de-offsetted for the remaining piping consumption $P^*_{cal} = P^m_{cal} \cdot c_w / c_{w,cal} - P_d$. As it can be seen from the figure, the model successfully captures the FCU dynamics. The comparison between calculated water side thermal power $P_{w,i}$ and air side thermal power $P_{a,i}$ for one selected FCU operating in a cooling season is given in Fig. 14.

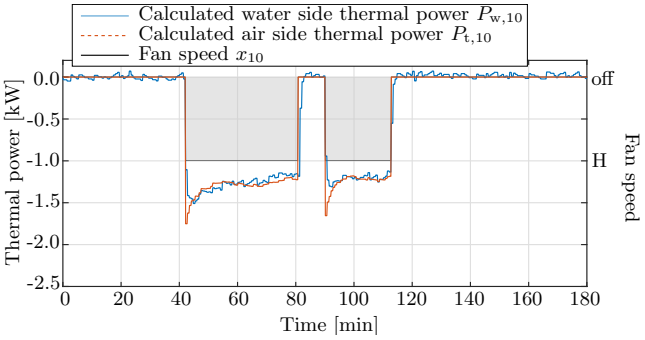

Fig. 14: The comparison between calculated air and water side thermal power for FCU i=10.

The estimated functional dependence $U_o(x, q_w)$ for three non-zero fan speeds of Trane FCC06 is shown in Fig. 15. In Fig. 16, normalized root mean squared error (NRMSE) of model return temperature response compared with minutely sampled

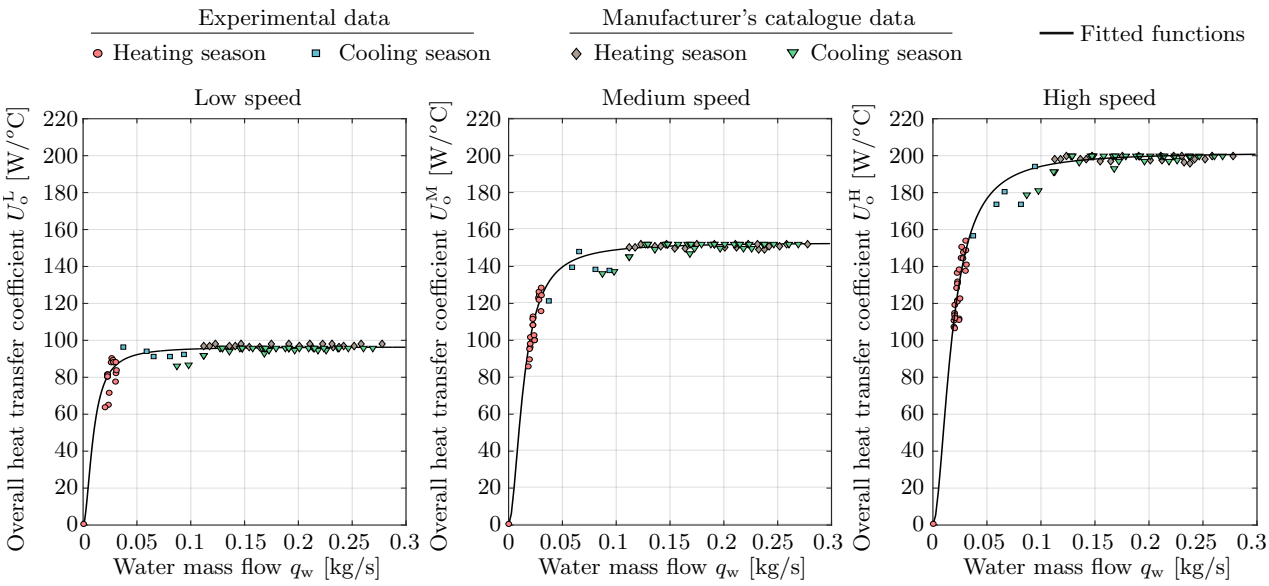

Fig. 15: Identified heat transfer coefficient function for low, medium and high fan speed of Trane FCC06.

measurements is given. NRMSE is calculated as:

$$\text{NRMSE} = \frac{1}{\overline{T}_{\text{w},i}^{\text{out,m}}} \sqrt{\frac{\sum_{k=1}^{M_i} (T_{\text{w},i}^{\text{out,m}}(k) - T_{\text{w},i}^{\text{out}}(k))^2}{M_i}}, \quad (31)$$

where $\overline{T}_{\text{w},i}^{\text{out,m}} = \sum_{k=1}^{M_i} T_{\text{w},i}^{\text{out,m}}(k)/M_i$ is the mean value of return medium temperature taken over considered data samples for a particular i^{th} FCU, M_i is overall number of samples collected during the experiment on the particular FCU and k denotes the measurement sample.The prediction error is below 6% for all data sets, even for prediction of the system behaviour 1 h in advance ($M_i \geq 60$ samples).

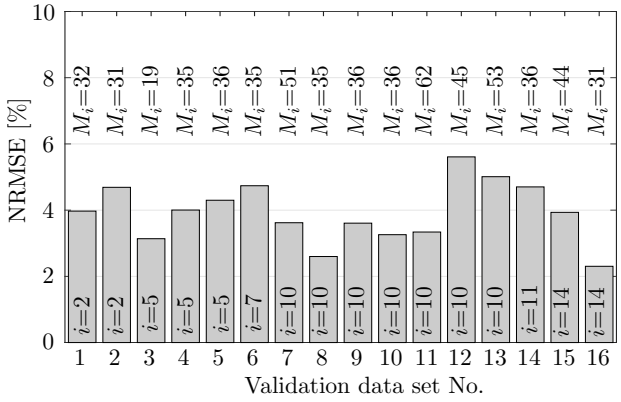

Fig. 16: NRMSE of the identified model return medium temperature response compared to the measurements for FCU $i = \{2, 5, 7, 10, 11, 14\}$.

VIII. Conclusion

A majority of modern commercial buildings are equipped with Building Energy Management Systems (BEMSs) to monitor and control different components of heating, ventilation, and air conditioning systems. This paper encloses a methodology for the development of a control-oriented energy model for a system of fan coil units, suitable for advanced model-based control algorithms. The developed models are validated on the experimental data collected from a 248-office living-lab. The proposed methodology stands out in its simplicity, cost-effectiveness (minimal sensor configuration), non-invasiveness and amount of time required for model identification. The incorporation of the developed energy model into the BEMS offers several advantages such as *i*) acquiring thermal powers per zone required for identification of building thermodynamic model, *ii*) estimation of unmeasured thermal loads affecting the zone for a very broad use in building monitoring and control, *iii*) usage of an advanced FCU control algorithm for direct control of thermal energy inputs per zone via fan speeds which makes it possible to realize optimized thermal energy inputs computed via predictive energy management schemes for maintaining zones thermal comfort and *iv*) development of fault detection and diagnosis algorithms for FCUs. The model error of both hydraulic and thermodynamic parts of the model is largely below 6% which is one of the most important conclusions of the paper about the applicability of the proposed identification methodology and presented model.

Acknowledgement

This work has been supported by the Croatian Science Foundation under the project No. 6731 - Control-based Hierarchical Consolidation of Large Consumers for Integration in Smart Grids (3CON, http://www.fer.unizg.hr/3con) and by the Danube Transnational Programme through the project Smart Building - Smart Grid - Smart City (3Smart, http://www.interreg-danube.eu/3smart), grant DTP1-502-3.2-3Smart. This research has been also supported by the European Regional Development Fund under the grant KK.01.1.1.01.0009 (DATACROSS). We also gratefully acknowledge the contribution of Elma Kurtalj company who provided us with Brightcore environment (https://brightcore.biz) for bidirectional building data communication.

APPENDIX

The minor losses in a pipe section include the losses in fittings, valves, diameter changes and other components that disturb the flow and it is represented in terms of l_{eq}/d ratio, where l_{eq} is the equivalent length of the straight pipe to give the same pressure drop as the fittings, and d is the inner diameter of fittings. The ratio for most common types of fittings used in heating/cooling installations is listed in Table A.1.

TABLE A.1: Equivalent length of fittings [40], [41].

Type of fitting	l_{eq}/d
Tee - along the straight	20
Tee - to the branch	60
Elbow 90 (smooth radius)	30
Three way valve (fully opened - through flow)	30
Sudden pipe diameter expansion	4*
Sudden pipe diameter contraction	20*

* used with inlet velocity.

REFERENCES

[1] International Energy Agency, "World energy outlook 2016," 2016. [Online]. Available: www.iea.org/publications/freepublications/publication/WorldEnergyOutlook2016ExecutiveSummaryEnglish.pdf

[2] *Europe's buildings under the microscope*. Buildings Performance Institute Europe, 2011. [Online]. Available: http://bpie.eu/wp-content/uploads/2015/10/HR_EU_B_under_microscope_study.pdf

[3] M. Gruber, A. Trüschel, and J.-O. Dalenbäck, "Model-based controllers for indoor climate control in office buildings - Complexity and performance evaluation," *Energy and Buildings*, vol. 68, pp. 213 – 222, 2014.

[4] M. Razmara, M. Maasoumy, M. Shahbakhti, and R. Robinett, "Optimal exergy control of building HVAC system," *Applied Energy*, vol. 156, pp. 555 – 565, 2015.

[5] A. Afram and F. Janabi-Sharifi, "Theory and applications of HVAC control systems - A review of model predictive control (MPC)," *Building and Environment*, vol. 72, pp. 343 – 355, 2014.

[6] M. Castilla, J. D. lvarez, J. E. Normey-Rico, and F. Rodríguez, "Thermal comfort control using a non-linear MPC strategy: A real case of study in a bioclimatic building," *Journal of Process Control*, vol. 24, no. 6, pp. 703–713, 2014.

[7] S. Prívara, J. Cigler, Z. Váňa, F. Oldewurtel, and E. Žáčeková, "Use of partial least squares within the control relevant identification for buildings," *Control Engineering Practice*, vol. 21, no. 1, pp. 113 – 121, 2013.

[8] D. Sturzenegger, D. Gyalistras, M. Morari, and R. S. Smith, "Model predictive climate control of a Swiss office building: Implementation, results, and cost-benefit analysis," *IEEE Transactions on Control Systems Technology*, vol. 24, no. 1, pp. 1–12, Jan 2016.

[9] M. Schmelas, T. Feldmann, and E. Bollin, "Savings through the use of adaptive predictive control of thermo-active building systems (TABS): A case study," *Applied Energy*, vol. 199, pp. 294 – 309, 2017.

[10] W. Liang, R. Quinte, X. Jia, and J.-Q. Sun, "MPC control for improving energy efficiency of a building air handler for multi-zone VAVs," *Building and Environment*, vol. 92, pp. 256 – 268, 2015.

[11] T. Y. Chen and A. K. Athienitis, "Investigation of practical issues in building thermal parameter estimation," *Building and Environment*, vol. 38, no. 8, pp. 1027 – 1038, 2003.

[12] P. Bacher and H. Madsen, "Identifying suitable models for the heat dynamics of buildings," *Energy and Buildings*, vol. 43, no. 7, pp. 1511–1522, 2011.

[13] B. Bueno, M. Street, T. Pflug, and C. Braesch, "A co-simulation modelling approach for the assessment of a ventilated double-skin complex fenestration system coupled with a compact fan-coil unit," *Energy and Buildings*, vol. 151, pp. 18 – 27, 2017.

[14] Y. Chen and S. Treado, "Development of a simulation platform based on dynamic models for HVAC control analysis," *Energy and Buildings*, vol. 68, pp. 376 – 386, 2014.

[15] L. Ratna Raju and T. K. Nandi, "Effective NTU of a counterflow heat exchanger with unbalanced flow and longitudinal heat conduction through fluid separating and outer walls," *Applied Thermal Engineering*, vol. 112, pp. 1172–1177, 2017.

[16] D. Rodríguez, G. Bejarano, J. A. Alfaya, M. G. Ortega, and F. Castaño, "Parameter identification of a multi-stage, multi-load-demand experimental refrigeration plant," *Control Engineering Practice*, vol. 60, pp. 133 – 147, 2017.

[17] A. Zavala-Río, C. Astorga-Zaragoza, and O. Hernández-González, "Bounded positive control for double-pipe heat exchangers," *Control Engineering Practice*, vol. 17, no. 1, pp. 136 – 145, 2009.

[18] S. Wongwises and Y. Chokeman, "Effect of fin pitch and number of tube rows on the air side performance of herringbone wavy fin and tube heat exchangers," *Energy Conversion and Management*, vol. 46, no. 13-14, pp. 2216–2231, 2005.

[19] D. Junqi, C. Jiangping, C. Zhijiu, Z. Yimin, and Z. Wenfeng, "Heat transfer and pressure drop correlations for the wavy fin and flat tube heat exchangers," *Applied Thermal Engineering*, vol. 27, no. 11, pp. 2066 – 2073, 2007.

[20] Y.-L. He, P. Chu, W.-Q. Tao, Y.-W. Zhang, and T. Xie, "Analysis of heat transfer and pressure drop for fin-and-tube heat exchangers with rectangular winglet-type vortex generators," *Applied Thermal Engineering*, vol. 61, no. 2, pp. 770–783, 2013.

[21] M. Jagirdar and P. S. Lee, "Mathematical modeling and performance evaluation of a desiccant coated fin-tube heat exchanger," *Applied Energy*, vol. 212, pp. 401–415, 2018.

[22] M. D'Antoni, D. Romeli, and R. Fedrizzi, "A model for the performance assessment of hybrid coolers by means of transient numerical simulation," *Applied Energy*, vol. 181, pp. 477–494, 2016.

[23] H. Maddah and N. Ghasemi, "Experimental evaluation of heat transfer efficiency of nanofluid in a double pipe heat exchanger and prediction of experimental results using artificial neural networks," *Heat and Mass Transfer*, vol. 53, no. 12, pp. 3459–3472, 2017.

[24] M. Mohanraj, S. Jayaraj, and C. Muraleedharan, "Applications of artificial neural networks for thermal analysis of heat exchangers - A review," *International Journal of Thermal Sciences*, vol. 90, pp. 150–172, 2015.

[25] K. S. Yigit and H. M. Ertunc, "Prediction of the air temperature and humidity at the outlet of a cooling coil using neural networks," *International Communications in Heat and Mass Transfer*, vol. 33, no. 7, pp. 898–907, 2006.

[26] C. Tan, J. Ward, S. Wilcox, and R. Payne, "Artificial neural network modelling of the thermal performance of a compact heat exchanger," *Applied Thermal Engineering*, vol. 29, no. 17, pp. 3609 – 3617, 2009.

[27] C. R. Ruivo and G. Angrisani, "Empirical component model to predict the overall performance of heating coils: Calibrations and tests based on manufacturer catalogue data," *Energy Conversion and Management*, vol. 89, pp. 749–763, 2015.

[28] Y. Shin, Y. S. Chang, and Y. Kim, "Controller design for a real-time air handling unit," *Control Engineering Practice*, vol. 10, no. 5, pp. 511 – 518, 2002.

[29] C. Ghiaus, A. Chicinas, and C. Inard, "Grey-box identification of air-handling unit elements," *Control Engineering Practice*, vol. 15, no. 4, pp. 421 – 433, 2007.

[30] J. Fernández-Seara, R. Diz, F. J. Uhía, and J. A. Dopazo, "Experimental analysis on pressure drop and heat transfer of a terminal fan-coil unit with ice slurry as cooling medium," *International Journal of Refrigeration*, vol. 33, no. 6, pp. 1095–1104, 2010.

[31] L. E. Ormsbee and D. J. Wood, "Explicit pipe network calibration," *Journal of Water Resources Planning and Management*, vol. 112, no. 2, pp. 166–182, 1986.

[32] M. Picón-Núñez, L. Canizalez-Dávalos, and G. T. Polley, "Modelling the thermo-hydraulic performance of cooling networks and its implications on design, operation and retrofit," in *Evaporation, Condensation and Heat Transfer*, A. Ahsan, Ed. Boston: InTech, 2011, pp. 189–206.

[33] X. Wang, W. Cai, and X. Yin, "A global optimized operation strategy for energy savings in liquid desiccant air conditioning using self-adaptive differential evolutionary algorithm," *Applied Energy*, vol. 187, pp. 410–423, 2017.

[34] Y.-W. Wang, W.-J. Cai, Y.-C. Soh, S.-J. Li, L. Lu, and L. Xie, "A simplified modeling of cooling coils for control and optimization of HVAC systems," *Energy Conversion and Management*, vol. 45, no. 1819, pp. 2915 – 2930, 2004.

[35] A. Martinčević, F. Rukavina, V. Lešić, and M. Vašak, "Comfort control in buildings with adherence to the required thermal energy input in zones," in *IEEE International Symposium on Industrial Electronics*, 2017, pp. 1477–1482.

[36] V. Lešić, A. Martinčević, and M. Vašak, "Modular energy cost optimization for buildings with integrated microgrid," *Applied Energy*, vol. 197, pp. 14 – 28, 2017.

[37] S. Pourarian, J. Wen, D. Veronica, A. Pertzborn, X. Zhou, and R. Liu, "A tool for evaluating fault detection and diagnostic methods for fan coil units," *Energy and Buildings*, vol. 136, pp. 151 – 160, 2017.

[38] F. Delmotte, M. Dambrine, S. Delrot, and S. Lalot, "Fouling detection in a heat exchanger: A polynomial fuzzy observer approach," *Control Engineering Practice*, vol. 21, no. 10, pp. 1386 – 1395, 2013.

[39] E. Weyer, G. Szederknyi, and K. Hangos, "Grey box fault detection of heat exchangers," *Control Engineering Practice*, vol. 8, no. 2, pp. 121 – 131, 2000.

[40] A. Kraus, J. Welty, and A. Aziz, "Flow in pipes and pipe networks," in *Introduction to Thermal and Fluid Engineering*. New York: Taylor & Francis, 2011, ch. 17, pp. 523–562.

[41] E. S. Menon and P. S. Menon, "Pressure loss through piping systems," in *Working Guide to Pumps and Pumping Stations*. Boston: Gulf Professional Publishing, 2010, pp. 69–112.

[42] MATLAB, *version 8.5.0 (R2015a)*. The MathWorks Inc., 2015.

[43] G.-Y. Jin, W.-J. Cai, Y.-W. Wang, and Y. Yao, "A simple dynamic model of cooling coil unit," *Energy Conversion and Management*, vol. 47, no. 1516, pp. 2659 – 2672, 2006.

[44] TRANE, Cooling and Heating Systems and Services, "Unitrane fan coil units (unt-prc006-e4)," 2010.